

# Evolution of superconducting order in $\text{Pr}(\text{Os}_{1-x}\text{Ru}_x)_4\text{Sb}_{12}$

Elbert E. M. Chia,\* M. B. Salamon, and D. Vandervelde

*Department of Physics, University of Illinois at Urbana-Champaign, 1110 W. Green St., Urbana IL 61801*

D. Kikuchi, H. Sugawara, and H. Sato

*Department of Physics, Tokyo Metropolitan University, Hachioji, Tokyo 192-0397, Japan*

(Dated: March 14, 2018)

We report measurements of the magnetic penetration depth  $\lambda$  in single crystals of  $\text{Pr}(\text{Os}_{1-x}\text{Ru}_x)_4\text{Sb}_{12}$  down to 0.1 K. Both  $\lambda$  and superfluid density  $\rho_s$  exhibit an exponential behavior for the  $x \geq 0.4$  samples, going from weak ( $x=0.4, 0.6$ ), to moderate, coupling ( $x=0.8$ ). For the  $x \leq 0.2$  samples, both  $\lambda$  and  $\rho_s$  vary as  $T^2$  at low temperatures, but  $\rho_s$  is  $s$ -wave-like at intermediate to high temperatures. Our data are consistent with a three-phase scenario, where a fully-gapped phase at  $T_{c1}$  undergoes two transitions: first to an unconventional phase at  $T_{c2} \lesssim T_{c1}$ , then to a nodal low- $T$  phase at  $T_{c3} < T_{c2}$ , for small values of  $x$ .

The recent discovery [1, 2] of the heavy Fermion (HF) skutterudite superconductor (SC)  $\text{PrOs}_4\text{Sb}_{12}$  has attracted much interest due to its differences with the other HFSC. Early work suggested that the ninefold degenerate  $J = 4$  Hund's rule multiplet of Pr is split by the cubic crystal electric field, such that its ground state is a *nonmagnetic*  $\Gamma_3$  doublet, separated from the first excited state  $\Gamma_5$  by  $\sim 10$  K. Hence its HF behavior, and consequently the origin of its superconductivity, might be attributed to the interaction between the electric quadrupolar moments of  $\text{Pr}^{3+}$  and the conduction electrons [1]. More recent results appear to rule this mechanism out, giving strong evidence for a singlet  $\Gamma_1$  ground state with a  $\Gamma_5$  triplet state at a slightly higher energy [3, 4]. In this scheme, aspherical Coulomb scattering [4] and spin-fluctuation scattering [5] have been proposed as mechanisms leading to superconductivity

Surprisingly, replacement of Os by Ru, i.e. in  $\text{PrRu}_4\text{Sb}_{12}$ , yields a superconductor with  $T_c \approx 1.25$  K [6] and significantly different properties. The effective mass of the heavy electrons calculated from de Haas-van Alphen (dHvA) and specific-heat measurements [1, 7] show that, while  $\text{PrOs}_4\text{Sb}_{12}$  is clearly a HF material,  $\text{PrRu}_4\text{Sb}_{12}$  is at most, a marginal HF. Various experimental results suggest that these two materials have different order-parameter symmetry. Firstly, there is no Hebel-Slichter peak in the nuclear quadrupole resonance (NQR) data [8] for  $\text{PrOs}_4\text{Sb}_{12}$ , while a distinct coherence peak was seen [9] in the Sb-NQR  $1/T_1$  data for  $\text{PrRu}_4\text{Sb}_{12}$ . Secondly, the low-temperature power-law behavior seen in specific heat [1] and penetration depth [10], and the angular variation of thermal conductivity [11], suggest the presence of nodes in the order parameter of  $\text{PrOs}_4\text{Sb}_{12}$ . Specifically, Refs. 10 and 11 reveal the presence of *point* nodes on the Fermi surface (FS). For  $\text{PrRu}_4\text{Sb}_{12}$ , however, exponential low-temperature behavior was seen in  $1/T_1$  [9] and penetration depth [12] data. The latter data were fit with an isotropic zero-temperature gap of magnitude  $\Delta(0) = 1.9k_B T_c$ , showing that  $\text{PrRu}_4\text{Sb}_{12}$  is a moderate-coupling superconduc-

tor. Thirdly, muon spin rotation ( $\mu\text{SR}$ ) experiments on  $\text{PrOs}_4\text{Sb}_{12}$  reveal the spontaneous appearance of static internal magnetic fields below  $T_c$ , providing evidence that the superconducting state is a time-reversal-symmetry-breaking (TRSB) state [13]. Such experiments have not been performed on  $\text{PrRu}_4\text{Sb}_{12}$ .

It is puzzling that the substitution of Ru for Os (same column in the periodic table) causes  $\text{PrRu}_4\text{Sb}_{12}$  to differ in so many respects from  $\text{PrOs}_4\text{Sb}_{12}$ , particularly if symmetry of the superconducting gap varies as we go from Os to Ru. Recently, Frederick *et al.* performed x-ray powder diffraction, magnetic susceptibility and electrical resistivity measurements [14] on single crystals of  $\text{Pr}(\text{Os}_{1-x}\text{Ru}_x)_4\text{Sb}_{12}$ . They found a smooth evolution of the lattice constant and  $T_c$  with  $x$ , albeit with a deep minimum (0.75 K) in  $T_c$  at  $x=0.6$ , and an increased splitting between the ground and excited states of the Pr ion. On the other hand, one still has to contend with measurements [10, 11, 13, 15] that indicate point-node gap structure, TRSB and a double superconducting transition  $T_{c2} \lesssim T_c$  [14] in  $\text{PrOs}_4\text{Sb}_{12}$ , none of which are seen for  $x > 0$ . We report here a complementary study of  $\text{Pr}(\text{Os}_{1-x}\text{Ru}_x)_4\text{Sb}_{12}$  using the penetration depth.

A recent paper [16] observed an unexpected enhancement of the lower critical field  $H_{c1}(T)$  and the critical current  $I_c(T)$  deep in the superconducting state below  $T \approx 0.6$  K ( $T/T_c \approx 0.3$ ) in  $\text{PrOs}_4\text{Sb}_{12}$ . They speculate that this reflects a transition into another superconducting phase that occurs below  $T_{c3} \approx 0.6$  K, and may explain anomalies in other measurements, such as the levelling off of Sb-NQR  $1/T_1$  below 0.6 K [9], the small downturn of penetration depth below 0.62 K and its deviation from point-node- $T^2$ -behavior above  $\sim 0.6$  K [10].

In this Letter, we present high-precision measurements of the penetration depth  $\lambda(T)$  of  $\text{Pr}(\text{Os}_{1-x}\text{Ru}_x)_4\text{Sb}_{12}$  ( $x=0.1, 0.2, 0.4, 0.6, 0.8$ ) at temperatures down to  $\sim 0.1$  K using the same experimental conditions as for  $\text{PrOs}_4\text{Sb}_{12}$  and  $\text{PrRu}_4\text{Sb}_{12}$  [10, 12]. For the  $x \geq 0.4$  samples, both  $\lambda(T)$  and superfluid density  $\rho_s(T)$  exhibit exponential behavior at low temperatures, supporting the presence of

an isotropic superconducting gap on the FS. The  $\rho_s(T)$  data agree with the theoretical curve over the entire temperature range. The values of  $\Delta(0)$  used in the fits suggest an increase in coupling strength from weak-coupling ( $x=0.4,0.6$ ) to moderate coupling ( $x=0.8$ ). On the other hand, the  $x \leq 0.2$  samples exhibit a low- $T$  power law, implying the existence of low-lying excitations. However, the  $\rho_s$  data fit a fully-gapped theoretical curve from intermediate temperatures up to  $T_c$ , but not curves based on a superconducting gap with line or point nodes. This is consistent with the scenario depicted by Cichorek *et al.* [16], where for the  $x \leq 0.2$ -samples, the fully-gapped high- $T$  phase undergoes a transition into a nodal low- $T$  phase below  $T_{c3}(x)$ . As  $x$  increases, the low- $T$  phase is suppressed ( $T_{c3}$  decreases) such that for the  $x \geq 0.4$ -samples,  $T_{c3}$  falls below the base temperature of our experiment, and we are left with a fully-gapped phase over our entire experimental temperature range. Taken together with other data, we suggest that, in addition to the two phases at  $T_{c1}$  and  $T_{c2}$ , there is a third superconducting phase at  $T_{c3}$  that exhibits point nodes.

The single crystal samples were grown by Sb self-flux method [6]. The observation of dHvA effect both in  $\text{PrOs}_4\text{Sb}_{12}$  and  $\text{PrRu}_4\text{Sb}_{12}$  could be an indirect evidence of high quality of these samples grown in the same manner. Measurements were performed utilizing a 21-MHz tunnel diode oscillator [17] with a noise level of 2 parts in  $10^9$  and low drift. The magnitude of the ac field is estimated to be less than 40 mOe. The sample was mounted, using a small amount of GE varnish, on a single crystal sapphire rod. The other end of the rod is thermally connected to the mixing chamber of an Oxford Kelvinox 25 dilution refrigerator. The sample temperature is monitored using a calibrated  $\text{RuO}_2$  resistor at low temperatures ( $T_{base} - 1.3$  K) and a calibrated Cernox thermometer at higher temperatures (1.2 K–1.8 K).

The deviation  $\Delta\lambda(T) = \lambda(T) - \lambda(0.1 \text{ K})$  is proportional to the change in resonant frequency  $\Delta f(T)$  of the oscillator, with the proportionality factor  $G$  dependent on sample and coil geometries. We determine  $G$  for a pure Al single crystal by fitting the Al data to extreme non-local expressions and then adjust for relative sample dimensions [18]. Testing this approach on a single crystal of Pb, we found good agreement with conventional BCS expressions. The value of  $G$  obtained this way has an uncertainty of  $\pm 10\%$  because our samples have a rectangular, rather than square, basal area [19].

We first discuss the  $x \geq 0.4$  samples. Figure 1 (○) shows  $\Delta\lambda(T)$  for the three samples ( $x=0.4,0.6,0.8$ ) as a function of temperature in the low-temperature region. The insets show  $\Delta\lambda(T)$  for the entire temperature range. The onset of the superconducting transitions  $T_c^*$  are 0.81 K ( $x=0.6$ ) and 0.88 K ( $x=0.8$ ). These values are consistent with those of Ref. 14. We could not obtain  $T_c^*$  for the  $x=0.4$  sample as the ac losses were so large that oscillation was lost before  $T_c$  was reached; its large

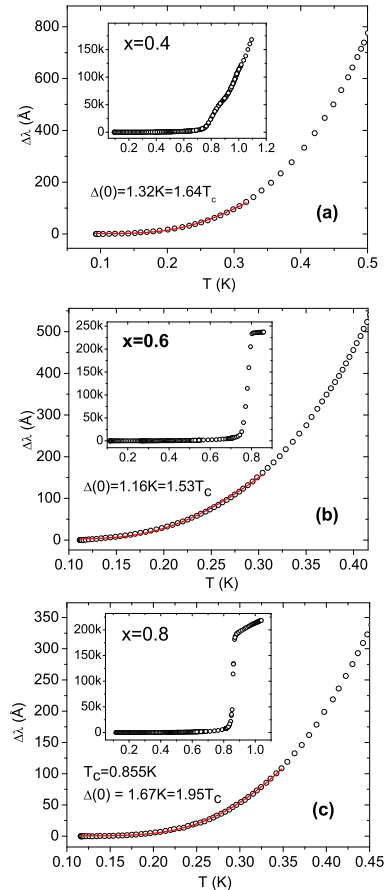


FIG. 1: (○) Low-temperature dependence of  $\Delta\lambda(T)$  for (a)  $x=0.4$ , (b)  $x=0.6$ , and (c)  $x=0.8$ . Lines: fits to BCS low- $T$  expression from  $T_{base}$  to  $0.4T_c$ . The parameters of the fits are described in the text. Insets show  $\Delta\lambda(T)$  over the full temperature range.

transition width is also consistent with the ac susceptibility data of Frederick *et al.* [14], though the origin is unknown. The values of  $T_c$ , determined from the point where the experimental superfluid density almost vanishes and fit the theoretical curves (described later), are 0.8 K ( $x=0.4$ ), 0.76 K ( $x=0.6$ ) and 0.86 K ( $x=0.8$ ).

For all three samples the data points flatten out below  $0.3T_c$ , implying activated behavior in this temperature range. We fit these data to the BCS low-temperature expression in the clean and local limit, from  $T_{base}$  ( $\sim 0.1$  K) to  $0.4T_c$ , using the expression  $\Delta\lambda(T) \propto \sqrt{\pi} \Delta(0) / 2k_B T \exp(-\Delta(0)/k_B T)$ , with the proportionality constant and  $\Delta(0)$  as parameters. The best fits (solid lines) are obtained when  $\Delta(0)/k_B T_c = 1.64$  ( $x=0.4$ ), 1.53 ( $x=0.6$ ) and 1.95 ( $x=0.8$ ). This implies that the  $x=0.4$  and  $0.6$  samples are weak-coupling, while the  $x=0.8$  sample is a moderate-coupling, superconductor. The  $x=0.8$  result is consistent with that for  $\text{PrRu}_4\text{Sb}_{12}$  ( $x=1$ ).

Sample $x$	0	0.1	0.2	0.4	0.6	0.8	1.0
$\Delta(0)/k_B T_c$	2.6	1.76	1.76	1.76	1.76	1.95	1.90
$\Delta C/C$	3.0	1.43	1.43	1.43	1.43	2.04	1.87
$\lambda(0)$ (nm)	344	320	380	340	380	400	290

TABLE I: Parameters used to calculate curves in Figs. 2 and 3. Values for  $x=0$  and  $x=1$  are included for comparison.

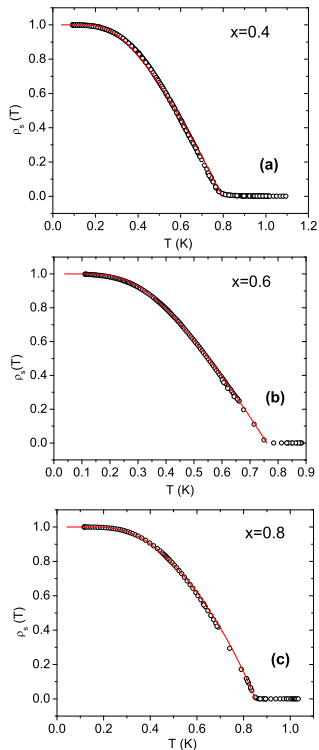


FIG. 2: (○) Superfluid density  $\rho_s(T) = [\lambda^2(0)/\lambda^2(T)]$  calculated from  $\Delta\lambda(T)$  data in Fig. 1, for (a)  $x=0.4$ , (b)  $x=0.6$ , and (c)  $x=0.8$ . Lines: Theoretical  $\rho_s(T)$  with parameters  $\Delta(0)/k_B T_c$  and  $\Delta C/\gamma T_c$  mentioned in the text.

To extract the superfluid density  $\rho_s$  from our data, we need to know  $\lambda(0)$ . Absent published data on  $\lambda(0)$ , we assume that it lies in the vicinity of 344 nm (for  $\text{PrOs}_4\text{Sb}_{12}$ ) [20] and 290 nm (for  $\text{PrRu}_4\text{Sb}_{12}$ ) [12]. We compute  $\rho_s$  for an isotropic  $s$ -wave superconductor in the clean and local limits using  $\rho_s = 1 + 2 \int_0^\infty \frac{\partial f}{\partial E} d\varepsilon$ , where  $f = [\exp(E/k_B T) + 1]^{-1}$  is the Fermi function, and  $E = [\varepsilon^2 + \Delta(T)^2]^{1/2}$  is the quasiparticle energy. The temperature-dependence of  $\Delta(T)$  can be obtained by using [21]  $\Delta(T) = \delta_{sc} k_B T_c \tanh\{(\pi/\delta_{sc}) \sqrt{(2/3)[(\Delta C)/C][(T_c/T) - 1]}\}$ , where  $\delta_{sc} \equiv \Delta(0)/k_B T_c$  is the only variable parameter. The specific heat jump  $\Delta C/C$  can be obtained from  $\Delta(0)/k_B T_c$  using strong-coupling equations [22, 23].

Fig. 2 shows the experimental (○) and calculated (solid line) values of  $\rho_s$  as a function of temperature for the  $x \geq 0.4$  samples. The theoretical curves fit the data very well using the parameters shown in Table I. Fitted values for  $\lambda(0)$  are reasonable, considering the uncertainty in

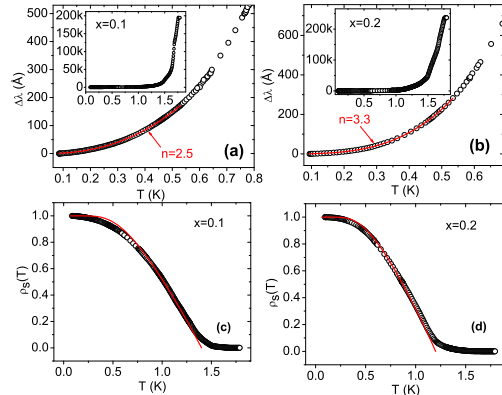


FIG. 3: (○) Low-temperature  $\Delta\lambda(T)$  for (a)  $x=0.1$  and (b)  $x=0.2$ . Lines: fits to  $\Delta\lambda(T) = A + BT^n$  from 0.1 K to 0.53 K. Insets show  $\Delta\lambda(T)$  over the full temperature range. (○) Superfluid density  $\rho_s(T)$  calculated from  $\Delta\lambda(T)$  data for (c)  $x=0.1$  and (d)  $x=0.2$ . Lines: Theoretical  $\rho_s(T)$  with weak-coupling parameters. Note the deviation of data from the theoretical curve at low temperatures is more pronounced for  $x=0.1$  than for  $x=0.2$ .

obtaining the calibration factor  $G$ .

We now turn to the  $x \leq 0.2$ -samples. Figs. 3a and 3b show  $\Delta\lambda(T)$  in the low-temperature region. The insets show  $\Delta\lambda(T)$  for the entire temperature range.  $T_c^*$  is measured to be 1.76 K ( $x=0.1$ ) and 1.77 K ( $x=0.2$ ), while  $T_c$  is 1.4 K ( $x=0.1$ ) and 1.2 K ( $x=0.2$ ). A fit of the low-temperature data (up to 0.53 K  $\approx 0.3T_c^*$ ) to a variable power law  $\Delta\lambda(T) = A + BT^n$  yields  $n=2.5$  ( $x=0.1$ ) and 3.3 ( $x=0.2$ ), indicative of low-lying excitations and incompatible with an isotropic gap.

Figs. 3c and 3d show the experimental (○) values of  $\rho_s(T)$ . The solid lines represent the theoretical curve based on an isotropic weak-coupling gap as in Table I. Note that the data do not agree with the theoretical curve at low temperatures, but agree from intermediate temperatures up to near  $T_c$ . The deviation of data from the theoretical curve at low temperatures is more pronounced for  $x=0.1$  than for  $x=0.2$ . This is consistent with the scenario depicted by Cichorek *et al.* [16], where for these low- $x$  samples, the fully-gapped high- $T$  phase undergoes a transition into a nodal low- $T$  phase below  $T_{c3}(x)$ . Our data also agree with the theory of Hotta [5], which predicts that when the  $\Gamma_1$ - $\Gamma_5$  spacing increases (observed as  $x$  is increased from 0 to 1 [14], and for  $x=1$  [6]), superconductivity changes from unconventional to conventional. We assume that this nodal phase is a *point-node* one, consistent with Refs. 10, 11, and so  $\Delta\lambda \propto T^2$  in this phase. Consequently, we plot  $\Delta\lambda(T)$  vs  $T^2$ , shown in Fig. 4a and 4b.  $T_{c3}(x)$  is determined from the temperature where the data deviate from linearity, from which we obtain  $T_{c3}(x=0.1) \approx 0.32 \pm 0.02$  K and  $T_{c3}(x=0.2) = 0.15 \pm 0.02$  K. Together with  $T_{c3}(x=0) \approx 0.61 \pm 0.01$  K deduced in Ref. 16 and 10, we plot  $T_{c3}$  vs  $x$  in Fig. 4c. We see that  $T_{c3}$

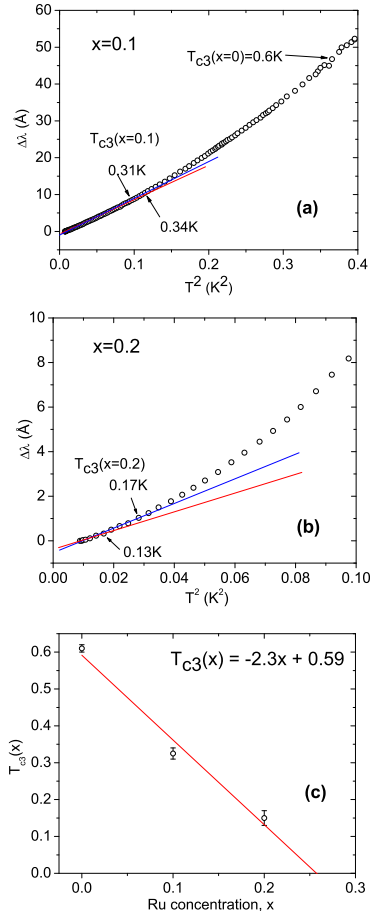


FIG. 4: (○) Low-temperature  $\Delta\lambda(T)$  vs  $T^2$  for (a)  $x=0.1$  and (b)  $x=0.2$ . The solid lines are visual aids to determining the range of linear fit.  $T_{c3}$  is defined to be the temperature where  $\Delta\lambda(T)$  starts to depart from  $T^2$ -behavior. (c) (○)  $T_{c3}(x)$  for  $x=0,0.1,0.2$ . Line: Best linear fit to the three data points. Note that the line extrapolates to zero near  $x=0.26$ .

varies linearly with  $x$ . Extrapolating the best-fit line yields  $T_{c3} \approx 0$  when  $x \approx 0.26$ . This implies that the low- $T$  nodal phase disappears, perhaps at a quantum critical point, when  $x \gtrsim 0.3$ , i.e. one only sees a fully-gapped behavior over the whole temperature range, agreeing with our  $x \geq 0.4$  data sets.

The continuity across the series of the first superconducting transition, that we label  $T_{c1}$ , and the BCS-like behavior of  $\rho_s$  over much of the  $T$ - $x$  plane, suggest that conventional phonon-mediated superconductivity prevails. Nonetheless, there is ample evidence for a second superconducting transition at  $T_{c2}$  at  $x=0$  below which unconventional superconductivity appears. Specific heat measurements on  $\text{Pr}_{1-y}\text{La}_y\text{Os}_4\text{Sb}_{12}$  [24] showed that the second superconducting transition at  $T_{c2}$  disappears between  $y=0.05$  and  $0.1$ , leaving conventional superconductivity for larger values of  $y$ . Figs. 1a, 3a

and 3b show some changes in curvature in  $\Delta\lambda$  close to  $T_c^*$  for the  $x=0.1, 0.2$  and  $0.4$  samples that could be indicative of  $T_{c2}$ , but which are not reproducible from sample to sample. As noted in the introductory paragraph, two mechanisms — spin-fluctuation and aspherical Coulomb scattering — have been proposed to explain the heavy-fermion behavior and superconducting properties of the  $x=0$  skutterudite. One possibility is that the spin-fluctuation mechanism is active at high temperatures where the  $\Gamma_5$  state is thermally populated on the Os-rich end of the phase diagram, but is suppressed by decreasing temperature or as Ru doping increases the  $\Gamma_1$ - $\Gamma_5$  splitting. Aspherical Coulomb scattering may remain important at lower temperatures and at larger values of  $x$ . Our data, when considered together with other data and theory, suggest *three* different superconducting phases: phonon-driven (conventional) across the series at the upper transition  $T_{c1}$ , but with spin-fluctuation and aspherical Coulomb scattering at the Os end giving rise to transitions to unconventional phases at  $T_{c2}$  and  $T_{c3}$ .

In conclusion, we report measurements of the magnetic penetration depth  $\lambda$  in single crystals of  $\text{Pr}(\text{Os}_{1-x}\text{Ru}_x)_4\text{Sb}_{12}$  down to  $\sim 0.1$  K. Both  $\lambda$  and superfluid density  $\rho_s$  exhibit an exponential behavior for the  $x \geq 0.4$  samples, going from weak-coupling ( $x=0.4, 0.6$ ) to moderate-coupling ( $x=0.8$ ). For the  $x \leq 0.2$  samples, both  $\lambda$  and  $\rho_s$  vary as  $T^2$  at low temperatures, but  $\rho_s$  is  $s$ -wave-like at intermediate to high temperatures. Our data are consistent with a three-phase scenario, where a fully-gapped phase at  $T_{c1}$  undergoes a transition to an unconventional phase at  $T_{c2} \approx T_{c1}$ , then to a nodal low- $T$  phase at  $T_{c3}$  for small values of  $x$ . The  $x$ -dependence of  $T_{c3}$  suggests that the low- $T$  phase disappears near  $x=0.3$ .

This material is based upon work supported by the U.S. Department of Energy, Division of Materials Sciences under Award No. DEFG02-91ER45439, through the Frederick Seitz Materials Research Laboratory at the University of Illinois at Urbana-Champaign, and the Grant-in-Aid for Scientific Research on the Priority Area “Skutterudites” (No. 15072206) from MEXT in Japan. Research for this publication was carried out in the Center for Microanalysis of Materials, University of Illinois at Urbana-Champaign.

\* Los Alamos National Laboratory, Los Alamos, New Mexico 87545, USA

- [1] E. D. Bauer *et al.*, Phys. Rev. B **65**, 100506(R) (2002).
- [2] M. B. Maple *et al.*, J. Phys. Soc. Jpn., Suppl. B **71**, 23 (2002).
- [3] Y. Aoki *et al.*, J. Phys. Soc. Jpn. **71**, 2098 (2002).
- [4] E. A. Goremychkin *et al.*, Phys. Rev. Lett. **93**, 157003 (2004).
- [5] T. Hotta, cond-mat/0410100.
- [6] N. Takeda and M. Ishikawa, J. Phys. Soc. Jpn. **69**, 868 (2000).
- [7] H. Sugawara *et al.*, Phys. Rev. B **66**, 220504(R) (2002).

- [8] H. Kotegawa *et al.*, Phys. Rev. Lett. **90**, 027001 (2003).
- [9] M. Yogi *et al.*, Phys. Rev. B **67**, 180501(R) (2003).
- [10] E. E. M. Chia, M. B. Salamon, H. Sugawara, and H. Sato, Phys. Rev. Lett. **91**, 247003 (2003).
- [11] K. Izawa *et al.*, Phys. Rev. Lett. **90**, 117001 (2003).
- [12] E. E. M. Chia, M. B. Salamon, H. Sugawara, and H. Sato, Phys. Rev. B **69**, 180509(R) (2004).
- [13] Y. Aoki *et al.*, Phys. Rev. Lett. **91**, 067003 (2003).
- [14] N. A. Frederick *et al.*, Phys. Rev. B **69**, 024523 (2004).
- [15] R. Vollmer *et al.*, Phys. Rev. Lett. **90**, 057001 (2003).
- [16] T. Cichorek *et al.*, cond-mat/0409331 .
- [17] I. Bonalde *et al.*, Phys. Rev. Lett. **85**, 4775 (2000).
- [18] E. E. M. Chia *et al.*, Phys. Rev. B **67**, 014527 (2003).
- [19] R. Prozorov, R. W. Giannetta, A. Carrington, and F. M. Araujo-Moreira, Phys. Rev. B **62**, 115 (2000).
- [20] D. E. MacLaughlin *et al.*, Phys. Rev. Lett. **89**, 157001 (2002).
- [21] F. Gross *et al.*, Z. Phys. B **64**, 175 (1986).
- [22] T. P. Orlando, E. J. McNiff, S. Foner, and M. R. Beasley, Phys. Rev. B **19**, 4545 (1979).
- [23] V. Z. Kresin and V. P. Parkhomenko, Sov. Phys.- Solid State **16**, 2180 (1975).
- [24] C. R. Rotundu, P. Kumar, and B. Andraka, cond-mat/0402599 .